



Measurement of Form-Factor-Independent Observables in the Decay $B^0 \rightarrow K^{*0} \mu^+ \mu^-$

R. Aaij *et al.**

(LHCb Collaboration)

(Received 9 August 2013; published 4 November 2013)

We present a measurement of form-factor-independent angular observables in the decay $B^0 \rightarrow K^{*0} \mu^+ \mu^-$. The analysis is based on a data sample corresponding to an integrated luminosity of 1.0 fb^{-1} , collected by the LHCb experiment in pp collisions at a center-of-mass energy of 7 TeV. Four observables are measured in six bins of the dimuon invariant mass squared q^2 in the range $0.1 < q^2 < 19.0 \text{ GeV}^2/c^4$. Agreement with recent theoretical predictions of the standard model is found for 23 of the 24 measurements. A local discrepancy, corresponding to 3.7 Gaussian standard deviations is observed in one q^2 bin for one of the observables. Considering the 24 measurements as independent, the probability to observe such a discrepancy, or larger, in one is 0.5%.

DOI: [10.1103/PhysRevLett.111.191801](https://doi.org/10.1103/PhysRevLett.111.191801)

PACS numbers: 13.20.He, 11.30.Rd, 12.60.-i

The rare decay $B^0 \rightarrow K^{*0} \mu^+ \mu^-$, where K^{*0} indicates the $K^{*0}(892) \rightarrow K^+ \pi^-$ decay, is a flavor-changing neutral current process that proceeds via loop and box amplitudes in the standard model (SM). In extensions of the SM, contributions from new particles can enter in competing amplitudes and modify the angular distributions of the decay products. This decay has been widely studied from both theoretical [1–4] and experimental [5–8] perspectives. Its angular distribution is described by three angles (θ_ℓ , θ_K , and ϕ) and the dimuon invariant mass

squared q^2 , θ_ℓ is the angle between the flight direction of the μ^+ (μ^-) and the B^0 (\bar{B}^0) meson in the dimuon rest frame, θ_K is the angle between the flight direction of the charged kaon and the B^0 (\bar{B}^0) meson in the K^{*0} (\bar{K}^{*0}) rest frame, and ϕ is the angle between the decay planes of the K^{*0} (\bar{K}^{*0}) and the dimuon system in the B^0 (\bar{B}^0) meson rest frame. A formal definition of the angles can be found in Ref. [8]. Using the definitions of Ref. [2] and summing over B^0 and \bar{B}^0 mesons, the differential angular distribution can be written as

$$\frac{1}{d\Gamma/dq^2} \frac{d^4\Gamma}{d\cos\theta_\ell d\cos\theta_K d\phi dq^2} = \frac{9}{32\pi} \left[\frac{3}{4}(1 - F_L)\sin^2\theta_K + F_L\cos^2\theta_K + \frac{1}{4}(1 - F_L)\sin^2\theta_K \cos 2\theta_\ell \right. \\ \left. - F_L\cos^2\theta_K \cos 2\theta_\ell + S_3\sin^2\theta_K \sin^2\theta_\ell \cos 2\phi + S_4 \sin 2\theta_K \sin 2\theta_\ell \cos\phi \right. \\ \left. + S_5 \sin 2\theta_K \sin\theta_\ell \cos\phi + S_6 \sin^2\theta_K \cos\theta_\ell + S_7 \sin 2\theta_K \sin\theta_\ell \sin\phi \right. \\ \left. + S_8 \sin 2\theta_K \sin 2\theta_\ell \sin\phi + S_9 \sin^2\theta_K \sin^2\theta_\ell \sin 2\phi \right], \quad (1)$$

where the q^2 dependent observables F_L and S_i are bilinear combinations of the K^{*0} decay amplitudes. These in turn are functions of the Wilson coefficients, which contain information about short distance effects and are sensitive to physics beyond the SM, and form factors, which depend on long distance effects. Combinations of F_L and S_i with reduced form-factor uncertainties have been proposed independently by several authors [3,4,9–11]. In particular, in the large recoil limit (low- q^2) the observables denoted as P'_4 , P'_5 , P'_6 , and P'_8 [12] are largely free from form-factor uncertainties. These observables are defined as

$$P'_{i=4,5,6,8} = \frac{S_{j=4,5,7,8}}{\sqrt{F_L(1 - F_L)}}. \quad (2)$$

This Letter presents the measurement of the observables $S_{j=4,5,7,8}$ and the respective observables $P'_{i=4,5,6,8}$. This is the first measurement of these quantities by any experiment. Moreover, these observables provide complementary information about physics beyond the SM with respect to the angular observables previously measured in this decay [5–8]. The data sample analyzed corresponds to an integrated luminosity of 1.0 fb^{-1} of pp collisions at a center-of-mass energy of 7 TeV collected by the LHCb experiment in 2011. Charge conjugation is implied throughout this Letter, unless otherwise stated.

The LHCb detector [13] is a single-arm forward spectrometer covering the pseudorapidity range $2 < \eta < 5$, designed for the study of particles containing b or c quarks.

*Full author list given at end of the article.

Published by the American Physical Society under the terms of the [Creative Commons Attribution 3.0 License](https://creativecommons.org/licenses/by/3.0/). Further distribution of this work must maintain attribution to the author(s) and the published article's title, journal citation, and DOI.

The detector includes a high-precision tracking system consisting of a silicon-strip vertex detector surrounding the pp interaction region, a large-area silicon-strip detector located upstream of a dipole magnet with a bending power of approximately 4 Tm, and three stations of silicon-strip detectors and straw drift tubes placed downstream of the magnet. The combined tracking system provides a momentum measurement with relative uncertainty that varies from 0.4% at 5 GeV/ c to 0.6% at 100 GeV/ c , and an impact parameter resolution of 20 μm for tracks with high transverse momentum (p_T). Charged hadrons are identified using two ring-imaging Cherenkov detectors [14]. Muons are identified by a system composed of alternating layers of iron and multiwire proportional chambers [15].

The trigger [16] consists of a hardware stage, based on information from the calorimeter and muon systems, followed by a software stage, which applies a full event reconstruction. Candidates for this analysis are required to pass a hardware trigger that selects events with at least one muon with $p_T > 1.48$ GeV/ c . In the software trigger, at least one of the final state particles is required to have both $p_T > 1.0$ GeV/ c and impact parameter larger than 100 μm with respect to all of the primary pp interaction vertices in the event. Finally, the tracks of two or more of the final state particles are required to form a vertex that is significantly displaced from the primary vertex.

Simulated events are used in several stages of the analysis, pp collisions are generated using PYTHIA 6.4 [17] with a specific LHCb configuration [18]. Decays of hadronic particles are described by EVTGEN [19], in which final state radiation is generated using PHOTOS [20]. The interaction of the generated particles with the detector and its response are implemented using the GEANT4 toolkit [21] as described in Ref. [22]. This analysis uses the same selection and acceptance correction technique as described in Ref. [8].

Signal candidates are required to pass a preselection that rejects a large fraction of background: the B^0 vertex is required to be well separated from the primary pp interaction point; the impact parameter with respect to the primary pp interaction point is required to be small for the B^0 candidate and large for the final state particles; and the angle between the B^0 momentum and the vector from the primary vertex to the B^0 decay vertex is required to be small. Finally, the reconstructed invariant mass of the K^{*0} candidate is required to be in the range $792 < m_{K\pi} < 992$ MeV/ c^2 . To further reject combinatorial background events, a boosted decision tree [23] using the AdaBoost algorithm [24] is applied. The boosted decision tree combines kinematic and geometrical properties of the event.

Several sources of peaking background have been considered. The decays $B^0 \rightarrow J/\psi K^{*0}$ and $B^0 \rightarrow \psi(2S)K^{*0}$, where the charmonium resonances decay into a muon pair, are rejected by vetoing events for which the dimuon system has an invariant mass ($m_{\mu\mu}$) in the range

2946–3176 MeV/ c^2 or 3586–3766 MeV/ c^2 . Both vetoes are extended downward by 150 MeV/ c^2 for B^0 candidates with invariant mass ($m_{K\pi\mu\mu}$) in the range 5150–5230 MeV/ c^2 to account for the radiative tails of the charmonium resonances. They are also extended upward by 25 MeV/ c^2 for candidates with $5370 < m_{K\pi\mu\mu} < 5470$ MeV/ c^2 , to account for non-Gaussian reconstruction effects. Backgrounds from $B^0 \rightarrow J/\psi K^{*0}$ decays with the kaon or pion from the K^{*0} decay and one of the muons from the J/ψ meson being misidentified and swapped with each other, are rejected by assigning the muon mass hypothesis to the K^+ or π^- and vetoing candidates for which the resulting invariant mass is in the range $3036 < m_{\mu\mu} < 3156$ MeV/ c^2 . Background from $B_s^0 \rightarrow \phi(\rightarrow K^+K^-)\mu^+\mu^-$ decays is removed by assigning the kaon mass hypothesis to the pion candidate and rejecting events for which the resulting invariant mass K^+K^- is consistent with the ϕ mass. A similar veto is applied to remove $\Lambda_b^0 \rightarrow \Lambda(1520)(\rightarrow pK^-)\mu^+\mu^-$ events. After these vetoes, the remaining peaking background is estimated to be negligibly small by using the simulation. It has been verified with the simulation that these vetoes do not bias the angular observables. In total, 883 signal candidates are observed in the range $0.1 < q^2 < 19.0$ GeV $^2/c^4$, with a signal over background ratio of about 5.

Detector acceptance effects are accounted for by weighting the candidates with the inverse of their efficiency. The efficiency is determined as a function of the three angles and q^2 by using a large sample of simulated events and assuming factorization in the three angles. Possible non-factorizable acceptance effects are evaluated and found to be roughly at the level of one tenth of the statistical uncertainty; they have been included in the systematic uncertainties. A range of control channels has been used to verify the accuracy or to adjust the simulation. The decays $D^{*+} \rightarrow D^0(\rightarrow K^-\pi^+)\pi^+$ and $B^+ \rightarrow J/\psi(\rightarrow \mu^+\mu^-)K^+$ have been used to tune the performances of the particle identification variables. The decay $B^0 \rightarrow J/\psi K^{*0}$, which has the same final state as the signal, has been used to validate the whole analysis by measuring its angular observables and comparing it with the literature. Extensive comparison of the kinematic and geometrical distributions of the decay $B^0 \rightarrow J/\psi K^{*0}$ in the data and simulation has also been performed. Because of the limited number of signal candidates in this data set, we do not fit the data to the full differential distribution of Eq. (1). In Ref. [8], the data were “folded” at $\phi = 0$ ($\phi \rightarrow \phi + \pi$ for $\phi < 0$) to reduce the number of parameters in the fit, while canceling the terms containing $\sin\phi$ and $\cos\phi$. Here, similar folding techniques are applied to specific regions of the three-dimensional angular space to exploit the (anti) symmetries of the differential decay rate with respect to combinations of angular variables. This simplifies the differential decay rate without losing experimental sensitivity. This technique is discussed in more detail in Ref. [25].

The following sets of transformations are used to determine the observables of interest:

$$P'_4, S_4: \begin{cases} \phi \rightarrow -\phi & \text{for } \phi < 0 \\ \phi \rightarrow \pi - \phi & \text{for } \theta_\ell > \pi/2 \\ \theta_\ell \rightarrow \pi - \theta_\ell & \text{for } \theta_\ell > \pi/2, \end{cases} \quad (3)$$

$$P'_5, S_5: \begin{cases} \phi \rightarrow -\phi & \text{for } \phi < 0 \\ \theta_\ell \rightarrow \pi - \theta_\ell & \text{for } \theta_\ell > \pi/2, \end{cases} \quad (4)$$

$$P'_6, S_7: \begin{cases} \phi \rightarrow \pi - \phi & \text{for } \phi > \pi/2 \\ \phi \rightarrow -\pi - \phi & \text{for } \phi < -\pi/2 \\ \theta_\ell \rightarrow \pi - \theta_\ell & \text{for } \theta_\ell > \pi/2, \end{cases} \quad (5)$$

$$P'_8, S_8: \begin{cases} \phi \rightarrow \pi - \phi & \text{for } \phi > \pi/2 \\ \phi \rightarrow -\pi - \phi & \text{for } \phi < -\pi/2 \\ \theta_K \rightarrow \pi - \theta_K & \text{for } \theta_\ell > \pi/2 \\ \theta_\ell \rightarrow \pi - \theta_\ell & \text{for } \theta_\ell > \pi/2. \end{cases} \quad (6)$$

Each transformation preserves the first five terms and the corresponding S_i term in Eq. (1), and cancels the other angular terms. Thus, the resulting angular distributions depend only on F_L , S_3 , and one of the observables $S_{4,5,7,8}$.

Four independent likelihood fits to the B^0 invariant mass and the transformed angular distributions are performed to extract the observables P'_i and S_i . The signal invariant mass shape is parametrized with the sum of two Crystal Ball functions [26], where the parameters are extracted from the

fit to $B^0 \rightarrow J/\psi K^{*0}$ decays in data. The background invariant mass shape is parametrized with an exponential function, while its angular distribution is parametrized with the direct product of three second-order polynomials, dependent on ϕ , $\cos\theta_K$, and $\cos\theta_\ell$. The angular observables F_L and S_3 are allowed to vary in the angular fit and are treated as nuisance parameters in this analysis. Their fit values agree with Ref. [8].

The presence of a $K^+ \pi^-$ system in an S -wave configuration, due to a nonresonant contribution or to feed down from $K^+ \pi^-$ scalar resonances, results in additional terms in the differential angular distribution. Denoting the right-hand side of Eq. (1) by W_P , the differential decay rate takes the form

$$(1 - F_S)W_P + \frac{9}{32\pi}(W_S + W_{SP}), \quad (7)$$

where

$$W_S = \frac{2}{3}F_S \sin^2\theta_\ell \quad (8)$$

and W_{SP} is given by

$$\begin{aligned} & \frac{4}{3}A_S \sin^2\theta_\ell \cos\theta_K + A_S^{(4)} \sin\theta_K \sin 2\theta_\ell \cos\phi \\ & + A_S^{(5)} \sin\theta_K \sin\theta_\ell \cos\phi + A_S^{(7)} \sin\theta_K \sin\theta_\ell \sin\phi \\ & + A_S^{(8)} \sin\theta_K \sin 2\theta_\ell \sin\phi. \end{aligned} \quad (9)$$

The factor F_S is the fraction of the S -wave component in the K^{*0} mass window, and W_{SP} contains all the interference

TABLE I. Measurement of the observables $P'_{4,5,6,8}$ and $S_{4,5,7,8}$ in the six q^2 bins of the analysis. For the observables P'_i the measurement in the q^2 bin $1.0 < q^2 < 6.0 \text{ GeV}^2/c^4$, which is the theoretically preferred region at large recoil, is also reported. The first uncertainty is statistical and the second is systematic.

q^2 [GeV^2/c^4]	P'_4	P'_5	P'_6	P'_8
0.10–2.00	$0.00^{+0.26}_{-0.26} \pm 0.03$	$0.45^{+0.19}_{-0.22} \pm 0.09$	$-0.24^{+0.19}_{-0.22} \pm 0.05$	$-0.06^{+0.28}_{-0.28} \pm 0.02$
2.00–4.30	$-0.37^{+0.29}_{-0.26} \pm 0.08$	$0.29^{+0.39}_{-0.38} \pm 0.07$	$0.15^{+0.36}_{-0.38} \pm 0.05$	$-0.15^{+0.29}_{-0.28} \pm 0.07$
4.30–8.68	$-0.59^{+0.15}_{-0.12} \pm 0.05$	$-0.19^{+0.16}_{-0.16} \pm 0.03$	$-0.04^{+0.15}_{-0.15} \pm 0.05$	$0.29^{+0.17}_{-0.19} \pm 0.03$
10.09–12.90	$-0.46^{+0.20}_{-0.17} \pm 0.03$	$-0.79^{+0.16}_{-0.19} \pm 0.19$	$-0.31^{+0.23}_{-0.22} \pm 0.05$	$-0.06^{+0.23}_{-0.22} \pm 0.02$
14.18–16.00	$0.09^{+0.35}_{-0.27} \pm 0.04$	$-0.79^{+0.20}_{-0.13} \pm 0.18$	$-0.18^{+0.25}_{-0.24} \pm 0.03$	$-0.20^{+0.30}_{-0.25} \pm 0.03$
16.00–19.00	$-0.35^{+0.26}_{-0.22} \pm 0.03$	$-0.60^{+0.19}_{-0.16} \pm 0.09$	$0.31^{+0.38}_{-0.37} \pm 0.10$	$0.06^{+0.26}_{-0.27} \pm 0.03$
1.00–6.00	$-0.29^{+0.18}_{-0.16} \pm 0.03$	$0.21^{+0.20}_{-0.21} \pm 0.03$	$-0.18^{+0.21}_{-0.21} \pm 0.03$	$0.23^{+0.18}_{-0.19} \pm 0.02$
q^2 [GeV^2/c^4]	S_4	S_5	S_7	S_8
0.10–2.00	$0.00^{+0.12}_{-0.12} \pm 0.03$	$0.22^{+0.09}_{-0.10} \pm 0.04$	$-0.11^{+0.11}_{-0.11} \pm 0.03$	$-0.03^{+0.13}_{-0.12} \pm 0.01$
2.00–4.30	$-0.14^{+0.13}_{-0.12} \pm 0.03$	$0.11^{+0.14}_{-0.13} \pm 0.03$	$0.06^{+0.15}_{-0.15} \pm 0.02$	$-0.06^{+0.12}_{-0.12} \pm 0.02$
4.30–8.68	$-0.29^{+0.06}_{-0.06} \pm 0.02$	$-0.09^{+0.08}_{-0.08} \pm 0.01$	$-0.02^{+0.07}_{-0.08} \pm 0.04$	$0.15^{+0.08}_{-0.08} \pm 0.01$
10.09–12.90	$-0.23^{+0.09}_{-0.08} \pm 0.02$	$-0.40^{+0.08}_{-0.10} \pm 0.10$	$-0.16^{+0.11}_{-0.12} \pm 0.03$	$-0.03^{+0.10}_{-0.10} \pm 0.01$
14.18–16.00	$0.04^{+0.14}_{-0.08} \pm 0.01$	$-0.38^{+0.10}_{-0.09} \pm 0.09$	$-0.09^{+0.13}_{-0.14} \pm 0.01$	$-0.10^{+0.13}_{-0.12} \pm 0.02$
16.00–19.00	$-0.17^{+0.11}_{-0.09} \pm 0.01$	$-0.29^{+0.09}_{-0.08} \pm 0.04$	$0.15^{+0.16}_{-0.15} \pm 0.03$	$0.03^{+0.12}_{-0.12} \pm 0.02$

terms $A_S^{(i)}$ of the S wave with the K^{*0} transversity amplitudes as defined in Ref. [27]. In Ref. [8], F_S was measured to be less than 0.07 at 68% confidence level. The maximum value that the quantities $A_S^{(i)}$ can assume is a function of F_S and F_L [12]. The S -wave contribution is neglected in the fit to data, but its effect is evaluated and assigned as a systematic uncertainty using pseudoexperiments. A large number of pseudoexperiments with $F_S = 0.07$ and with the interference terms set to their maximum allowed values are generated. All other parameters, including the angular observables, are set to their measured values in the data. The pseudoexperiments are fitted ignoring S -wave and interference contributions. The corresponding bias in the measurement of the angular observables is assigned as a systematic uncertainty.

The results of the angular fits to the data are presented in Table I. The statistical uncertainties are determined using the Feldman-Cousins method [28]. The systematic uncertainty takes into account the limited knowledge of the angular acceptance, uncertainties in the signal and background invariant mass models, the angular model for the background, and the impact of a possible S -wave amplitude. A more detailed discussion of the systematic uncertainties can be found in Ref. [25]. Effects due to B^0/\bar{B}^0 production asymmetry have been considered and found negligibly small. The comparison between the measurements and the theoretical predictions from Ref. [10] are shown in Fig. 1 for the observables P'_4 and P'_5 . The observables P'_6 and P'_8 (as well as S_7 and S_8) are suppressed by the small size of the strong phase difference between the decay amplitudes, and therefore are expected to be close to 0 across the whole q^2 region.

In general, the measurements agree with SM expectations [12], apart from a sizeable discrepancy in the interval $4.30 < q^2 < 8.68 \text{ GeV}^2/c^4$ for the observable P'_5 . The p -value, calculated using pseudoexperiments, with respect to the upper bound of the theoretical predictions given in Ref. [12], for the observed deviation is 0.02%, corresponding to 3.7 Gaussian standard deviations (σ). If we consider the 24 measurements as independent, the probability that at least one varies from the expected value by 3.7σ or more is approximately 0.5%. A discrepancy of 2.5σ is observed integrating over the region $1.0 < q^2 < 6.0 \text{ GeV}^2/c^4$ (see Table I), which is considered the most robust region for theoretical predictions at large recoil. The discrepancy is also observed in the observable S_5 . The value of S_5 quantifies the asymmetry between decays with a positive and negative value of $\cos\theta_K$ for $|\phi| < \pi/2$, averaged with the opposite asymmetry of events with $|\phi| > \pi/2$ [2]. As a cross check, this asymmetry was also determined from a counting analysis. The result is consistent with the value for S_5 determined from the fit. It is worth noting that the predictions for the first two q^2 bins and for the region $1.0 < q^2 < 6.0 \text{ GeV}^2/c^4$ are also calculated in Ref. [29], where power corrections to the QCD factorization framework and

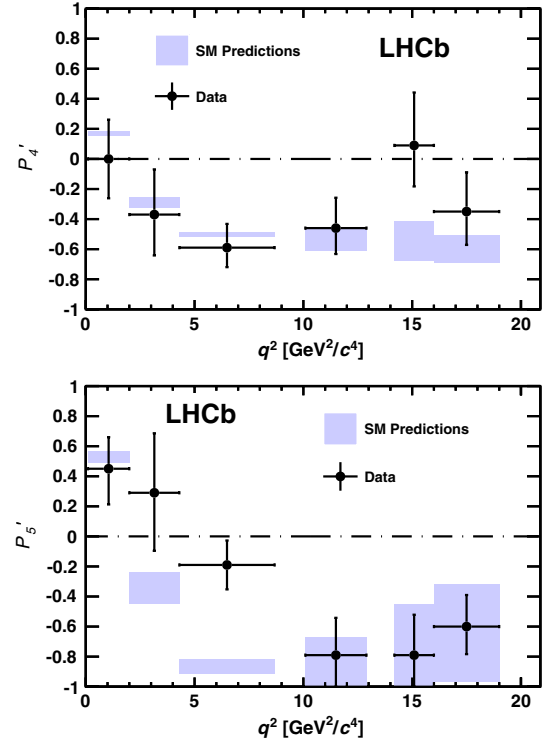


FIG. 1 (color online). Measured values of P'_4 and P'_5 (black points) compared with SM predictions from Ref. [10] [gray (blue) bands]. The error bars indicate in each case the 68.3% confidence level.

resonance contributions are considered. However, there is not yet consensus in the literature about the best approach to treat these power corrections. The technique used in Ref. [25] leads to a larger theoretical uncertainty with respect to Ref. [10].

In conclusion, we measure for the first time the angular observables S_4 , S_5 , S_7 , S_8 , and the corresponding form-factor-independent observables P'_4 , P'_5 , P'_6 , and P'_8 in the decay $B^0 \rightarrow K^{*0} \mu^+ \mu^-$. These measurements have been performed in six q^2 bins for each of the four observables. Agreement with SM predictions [10] is observed for 23 of the 24 measurements, while a local discrepancy of 3.7σ is observed in the interval $4.30 < q^2 < 8.68 \text{ GeV}^2/c^4$ for the observable P'_5 . Integrating over the region $1.0 < q^2 < 6.0 \text{ GeV}^2/c^4$, the observed discrepancy in P'_5 is 2.5σ . The observed discrepancy in the angular observable P'_5 could be caused by a smaller value of the Wilson coefficient C_9 with respect to the SM, as has been suggested to explain some other small inconsistencies between the $B^0 \rightarrow K^{*0} \mu^+ \mu^-$ data [6] and SM predictions [30]. Measurements with more data and further theoretical studies will be important to draw more definitive conclusions about this discrepancy.

We express our gratitude to our colleagues in the CERN accelerator departments for the excellent performance of the LHC. We thank the technical and administrative staff at the LHCb institutes. We acknowledge

support from CERN and from the national agencies: CAPES, CNPq, FAPERJ, and FINEP (Brazil); NSFC (China); CNRS/IN2P3 and Region Auvergne (France); BMBF, DFG, HGF and MPG (Germany); SFI (Ireland); INFN (Italy); FOM and NWO (The Netherlands); SCSR (Poland); MEN/IFA (Romania); MinES, Rosatom, RFBR and NRC “Kurchatov Institute” (Russia); MinECO, XuntaGal, and GENCAT (Spain); SNSF and SER (Switzerland); NAS Ukraine (Ukraine); STFC (U.K.); NSF (U.S.). We also acknowledge the support received from the ERC under FP7. The Tier1 computing centers are supported by IN2P3 (France), KIT and BMBF (Germany), INFN (Italy), NWO and SURF (The Netherlands), PIC (Spain), GridPP (U.K.). We are thankful for the computing resources put at our disposal by Yandex LLC (Russia), as well as to the communities behind the multiple open source software packages that we depend on.

-
- [1] F. Kruger, L. M. Sehgal, N. Sinha, and R. Sinha, *Phys. Rev. D* **61**, 114028 (2000).
- [2] W. Altmannshofer, P. Ball, A. Bharucha, A. J. Buras, D. M. Straub, and M. Wick, *J. High Energy Phys.* **01** (2009) 019.
- [3] D. Bečirević and E. Schneider, *Nucl. Phys.* **B854**, 321 (2012).
- [4] J. Matias, F. Mescia, M. Ramon, and J. Virto, *J. High Energy Phys.* **04** (2012) 104.
- [5] B. Aubert *et al.* (BABAR Collaboration), *Phys. Rev. D* **79**, 031102 (2009).
- [6] J.-T. Wei *et al.* (Belle Collaboration), *Phys. Rev. Lett.* **103**, 171801 (2009).
- [7] T. Aaltonen *et al.* (CDF Collaboration), *Phys. Rev. Lett.* **108**, 081807 (2012).
- [8] R. Aaij *et al.* (LHCb Collaboration), *J. High Energy Phys.* **08** (2013) 131.
- [9] F. Kruger and J. Matias, *Phys. Rev. D* **71**, 094009 (2005).
- [10] U. Egede, T. Hurth, J. Matias, M. Ramon, and W. Reece, *J. High Energy Phys.* **11** (2008) 032.
- [11] C. Bobeth, G. Hiller, and D. van Dyk, *J. High Energy Phys.* **07** (2011) 067.
- [12] S. Descotes-Genon, T. Hurth, J. Matias, and J. Virto, *J. High Energy Phys.* **05** (2013) 137.
- [13] A. A. Alves, Jr. *et al.* (LHCb Collaboration), *JINST* **3**, S08005 (2008).
- [14] M. Adinolfi *et al.*, *Eur. Phys. J. C* **73**, 2431 (2012).
- [15] A. A. Alves, Jr. *et al.*, *JINST* **8**, P02022 (2012).
- [16] R. Aaij *et al.*, *JINST* **8**, P04022 (2013).
- [17] T. Sjöstrand, S. Mrenna, and P. Skands, *J. High Energy Phys.* **05** (2006) 026.
- [18] I. Belyaev *et al.*, *Nucl. Sci. Symp. Conf. Rec.* 1155 (2010).
- [19] D. Lange, *Nucl. Instrum. Methods Phys. Res., Sect. A* **462**, 152 (2001).
- [20] P. Golonka and Z. Was, *Eur. Phys. J. C* **45**, 97 (2006).
- [21] J. Allison *et al.*, *IEEE Trans. Nucl. Sci.* **53**, 270 (2006); S. Agostinelli *et al.* (GEANT Collaboration), *Nucl. Instrum. Methods Phys. Res., Sect. A* **506**, 250 (2003).
- [22] M. Clemencic, G. Corti, S. Easo, C. R. Jones, S. Miglioranza, M. Pappagallo, and P. Robbe, *J. Phys. Conf. Ser.* **331**, 032023 (2011).
- [23] L. Breiman, J. H. Friedman, R. A. Olshen, and C. J. Stone, *Classification and Regression Trees* (Wadsworth International Group, Belmont, CA, 1984).
- [24] Y. Freund and R. E. Schapire, *J. Comput. Syst. Sci.* **55**, 119 (1997).
- [25] M. De Cian, Ph.D. thesis, University of Zurich, 2013 [Report No. CERN-THESIS-2013-145].
- [26] T. Skwarnicki, Ph.D. thesis, Institute of Nuclear Physics, Krakow, 1986 [Report No. DESY-F31-86-02].
- [27] J. Matias, *Phys. Rev. D* **86**, 094024 (2012).
- [28] G. J. Feldman and R. D. Cousins, *Phys. Rev. D* **57**, 3873 (1998).
- [29] S. Jäger and J. M. Camalich, *J. High Energy Phys.* **05** (2013) 043.
- [30] S. Descotes-Genon, J. Matias, and J. Virto, *Phys. Rev. D* **88**, 074002 (2013).
-

R. Aaij,⁴⁰ B. Adeva,³⁶ M. Adinolfi,⁴⁵ C. Adrover,⁶ A. Affolder,⁵¹ Z. Ajaltouni,⁵ J. Albrecht,⁹ F. Alessio,³⁷ M. Alexander,⁵⁰ S. Ali,⁴⁰ G. Alkhazov,²⁹ P. Alvarez Cartelle,³⁶ A. A. Alves, Jr.,^{24,37} S. Amato,² S. Amerio,²¹ Y. Amhis,⁷ L. Anderlini,^{17,f} J. Anderson,³⁹ R. Andreassen,⁵⁶ J. E. Andrews,⁵⁷ R. B. Appleby,⁵³ O. Aquines Gutierrez,¹⁰ F. Archilli,¹⁸ A. Artamonov,³⁴ M. Artuso,⁵⁸ E. Aslanides,⁶ G. Auremma,^{24,m} M. Baalouch,⁵ S. Bachmann,¹¹ J. J. Back,⁴⁷ C. Baesso,⁵⁹ V. Balagura,³⁰ W. Baldini,¹⁶ R. J. Barlow,⁵³ C. Barschel,³⁷ S. Barsuk,⁷ W. Barter,⁴⁶ Th. Bauer,⁴⁰ A. Bay,³⁸ J. Beddow,⁵⁰ F. Bedeschi,²² I. Bediaga,¹ S. Belogurov,³⁰ K. Belous,³⁴ I. Belyaev,³⁰ E. Ben-Haim,⁸ G. Bencivenni,¹⁸ S. Benson,⁴⁹ J. Benton,⁴⁵ A. Berezhnoy,³¹ R. Bernet,³⁹ M.-O. Bettler,⁴⁶ M. van Beuzekom,⁴⁰ A. Bien,¹¹ S. Bifani,⁴⁴ T. Bird,⁵³ A. Bizzeti,^{17,h} P. M. Bjørnstad,⁵³ T. Blake,³⁷ F. Blanc,³⁸ J. Blouw,¹¹ S. Blusk,⁵⁸ V. Bocci,²⁴ A. Bondar,³³ N. Bondar,²⁹ W. Bonivento,¹⁵ S. Borghi,⁵³ A. Borgia,⁵⁸ T. J. V. Bowcock,⁵¹ E. Bowen,³⁹ C. Bozzi,¹⁶ T. Brambach,⁹ J. van den Brand,⁴¹ J. Bressieux,³⁸ D. Brett,⁵³ M. Britsch,¹⁰ T. Britton,⁵⁸ N. H. Brook,⁴⁵ H. Brown,⁵¹ I. Burducea,²⁸ A. Bursche,³⁹ G. Busetto,^{21,q} J. Buytaert,³⁷ S. Cadeddu,¹⁵ O. Callot,⁷ M. Calvi,^{20,j} M. Calvo Gomez,^{35,n} A. Camboni,³⁵ P. Campana,^{18,37} D. Campora Perez,³⁷ A. Carbone,^{14,c} G. Carboni,^{23,k} R. Cardinale,^{19,i} A. Cardini,¹⁵ H. Carranza-Mejia,⁴⁹ L. Carson,⁵² K. Carvalho Akiba,² G. Casse,⁵¹ L. Castillo Garcia,³⁷ M. Cattaneo,³⁷ Ch. Cauet,⁹ R. Cenci,⁵⁷ M. Charles,⁵⁴ Ph. Charpentier,³⁷ P. Chen,^{3,38} N. Chiapolini,³⁹ M. Chrzaszcz,²⁵ K. Ciba,³⁷ X. Cid Vidal,³⁷ G. Ciezarek,⁵² P. E. L. Clarke,⁴⁹ M. Clemencic,³⁷

H. V. Cliff,⁴⁶ J. Closier,³⁷ C. Coca,²⁸ V. Coco,⁴⁰ J. Cogan,⁶ E. Cogneras,⁵ P. Collins,³⁷ A. Comerma-Montells,³⁵ A. Contu,^{15,37} A. Cook,⁴⁵ M. Coombes,⁴⁵ S. Coquereau,⁸ G. Corti,³⁷ B. Couturier,³⁷ G. A. Cowan,⁴⁹ D. C. Craik,⁴⁷ S. Cunliffe,⁵² R. Currie,⁴⁹ C. D'Ambrosio,³⁷ P. David,⁸ P. N. Y. David,⁴⁰ A. Davis,⁵⁶ I. De Bonis,⁴ K. De Bruyn,⁴⁰ S. De Capua,⁵³ M. De Cian,¹¹ J. M. De Miranda,¹ L. De Paula,² W. De Silva,⁵⁶ P. De Simone,¹⁸ D. Decamp,⁴ M. Deckenhoff,⁹ L. Del Buono,⁸ N. Déleage,⁴ D. Derkach,⁵⁴ O. Deschamps,⁵ F. Dettori,⁴¹ A. Di Canto,¹¹ H. Dijkstra,³⁷ M. Dogaru,²⁸ S. Donleavy,⁵¹ F. Dordei,¹¹ A. Dosil Suárez,³⁶ D. Dossett,⁴⁷ A. Dovbnya,⁴² F. Dupertuis,³⁸ P. Durante,³⁷ R. Dzhelyadin,³⁴ A. Dziurda,²⁵ A. Dzyuba,²⁹ S. Easo,⁴⁸ U. Egede,⁵² V. Egorychev,³⁰ S. Eidelman,³³ D. van Eijk,⁴⁰ S. Eisenhardt,⁴⁹ U. Eitschberger,⁹ R. Ekelhof,⁹ L. Eklund,^{50,37} I. El Rifai,⁵ Ch. Elsasser,³⁹ A. Falabella,^{14,e} C. Färber,¹¹ G. Fardell,⁴⁹ C. Farinelli,⁴⁰ S. Farry,⁵¹ D. Ferguson,⁴⁹ V. Fernandez Albor,³⁶ F. Ferreira Rodrigues,¹ M. Ferro-Luzzi,³⁷ S. Filippov,³² M. Fiore,¹⁶ C. Fitzpatrick,³⁷ M. Fontana,¹⁰ F. Fontanelli,^{19,i} R. Forty,³⁷ O. Francisco,² M. Frank,³⁷ C. Frei,³⁷ M. Frosini,^{17,f} S. Furcas,²⁰ E. Furfaro,^{23,k} A. Gallas Torreira,³⁶ D. Galli,^{14,c} M. Gandelman,² P. Gandini,⁵⁸ Y. Gao,³ J. Garofoli,⁵⁸ P. Garosi,⁵³ J. Garra Tico,⁴⁶ L. Garrido,³⁵ C. Gaspar,³⁷ R. Gauld,⁵⁴ E. Gersabeck,¹¹ M. Gersabeck,⁵³ T. Gershon,^{47,37} Ph. Ghez,⁴ V. Gibson,⁴⁶ L. Giubega,²⁸ V. V. Gligorov,³⁷ C. Göbel,⁵⁹ D. Golubkov,³⁰ A. Golutvin,^{52,30,37} A. Gomes,² P. Gorbounov,^{30,37} H. Gordon,³⁷ C. Gotti,²⁰ M. Grabalosa Gándara,⁵ R. Graciani Diaz,³⁵ L. A. Granado Cardoso,³⁷ E. Graugés,³⁵ G. Graziani,¹⁷ A. Grecu,²⁸ E. Greening,⁵⁴ S. Gregson,⁴⁶ P. Griffith,⁴⁴ O. Grünberg,⁶⁰ B. Gui,⁵⁸ E. Gushchin,³² Yu. Guz,^{34,37} T. Gys,³⁷ C. Hadjivasiliou,⁵⁸ G. Haefeli,³⁸ C. Haen,³⁷ S. C. Haines,⁴⁶ S. Hall,⁵² B. Hamilton,⁵⁷ T. Hampson,⁴⁵ S. Hansmann-Menzemer,¹¹ N. Harnew,⁵⁴ S. T. Harnew,⁴⁵ J. Harrison,⁵³ T. Hartmann,⁶⁰ J. He,³⁷ T. Head,³⁷ V. Heijne,⁴⁰ K. Hennessy,⁵¹ P. Henrard,⁵ J. A. Hernando Morata,³⁶ E. van Herwijnen,³⁷ M. Hess,⁶⁰ A. Hicheur,¹ E. Hicks,⁵¹ D. Hill,⁵⁴ M. Hoballah,⁵ C. Hombach,⁵³ P. Hopchev,⁴ W. Hulsbergen,⁴⁰ P. Hunt,⁵⁴ T. Huse,⁵¹ N. Hussain,⁵⁴ D. Hutchcroft,⁵¹ D. Hynds,⁵⁰ V. Iakovenko,⁴³ M. Idzik,²⁶ P. Ilten,¹² R. Jacobsson,³⁷ A. Jaeger,¹¹ E. Jans,⁴⁰ P. Jaton,³⁸ A. Jawahery,⁵⁷ F. Jing,³ M. John,⁵⁴ D. Johnson,⁵⁴ C. R. Jones,⁴⁶ C. Joram,³⁷ B. Jost,³⁷ M. Kaballo,⁹ S. Kandybei,⁴² W. Kalso,⁶ M. Karacson,³⁷ T. M. Karbach,³⁷ I. R. Kenyon,⁴⁴ T. Ketel,⁴¹ A. Keune,³⁸ B. Khanji,²⁰ O. Kochebina,⁷ I. Komarov,³⁸ R. F. Koopman,⁴¹ P. Koppenburg,⁴⁰ M. Korolev,³¹ A. Kozlinskiy,⁴⁰ L. Kravchuk,³² K. Kreplin,¹¹ M. Kreps,⁴⁷ G. Krocker,¹¹ P. Krokovny,³³ F. Kruse,⁹ M. Kucharczyk,^{20,25,j} V. Kudryavtsev,³³ K. Kurek,²⁷ T. Kvaratskheliya,^{30,37} V. N. La Thi,³⁸ D. Lacarrere,³⁷ G. Lafferty,⁵³ A. Lai,¹⁵ D. Lambert,⁴⁹ R. W. Lambert,⁴¹ E. Lanciotti,³⁷ G. Lanfranchi,¹⁸ C. Langenbruch,³⁷ T. Latham,⁴⁷ C. Lazzaroni,⁴⁴ R. Le Gac,⁶ J. van Leerdam,⁴⁰ J.-P. Lees,⁴ R. Lefèvre,⁵ A. Leflat,³¹ J. Lefrançois,⁷ S. Leo,²² O. Leroy,⁶ T. Lesiak,²⁵ B. Leverington,¹¹ Y. Li,³ L. Li Gioi,⁵ M. Liles,⁵¹ R. Lindner,³⁷ C. Linn,¹¹ B. Liu,³ G. Liu,³⁷ S. Lohn,³⁷ I. Longstaff,⁵⁰ J. H. Lopes,² N. Lopez-March,³⁸ H. Lu,³ D. Lucchesi,^{21,q} J. Luisier,³⁸ H. Luo,⁴⁹ F. Machefert,⁷ I. V. Machikhiliyan,^{4,30} F. Maciuc,²⁸ O. Maev,^{29,37} S. Malde,⁵⁴ G. Manca,^{15,d} G. Mancinelli,⁶ J. Maratas,⁵ U. Marconi,¹⁴ P. Marino,^{22,s} R. Märki,³⁸ J. Marks,¹¹ G. Martellotti,²⁴ A. Martens,⁸ A. Martín Sánchez,⁷ M. Martinelli,⁴⁰ D. Martinez Santos,⁴¹ D. Martins Tostes,² A. Martynov,³¹ A. Massafferri,¹ R. Matev,³⁷ Z. Mathe,³⁷ C. Matteuzzi,²⁰ E. Maurice,⁶ A. Mazurov,^{16,32,37,e} J. McCarthy,⁴⁴ A. McNab,⁵³ R. McNulty,¹² B. McSkelly,⁵¹ B. Meadows,^{56,54} F. Meier,⁹ M. Meissner,¹¹ M. Merk,⁴⁰ D. A. Milanes,⁸ M.-N. Minard,⁴ J. Molina Rodriguez,⁵⁹ S. Monteil,⁵ D. Moran,⁵³ P. Morawski,²⁵ A. Mordà,⁶ M. J. Morello,^{22,s} R. Mountain,⁵⁸ I. Mous,⁴⁰ F. Muheim,⁴⁹ K. Müller,³⁹ R. Muresan,²⁸ B. Muryn,²⁶ B. Muster,³⁸ P. Naik,⁴⁵ T. Nakada,³⁸ R. Nandakumar,⁴⁸ I. Nasteva,¹ M. Needham,⁴⁹ S. Neubert,³⁷ N. Neufeld,³⁷ A. D. Nguyen,³⁸ T. D. Nguyen,³⁸ C. Nguyen-Mau,^{38,o} M. Nicol,⁷ V. Niess,⁵ R. Niet,⁹ N. Nikitin,³¹ T. Nikodem,¹¹ A. Nomerotski,⁵⁴ A. Novoselov,³⁴ A. Oblakowska-Mucha,²⁶ V. Obraztsov,³⁴ S. Oggero,⁴⁰ S. Ogilvy,⁵⁰ O. Okhrimenko,⁴³ R. Oldeman,^{15,d} M. Orlandea,²⁸ J. M. Otalora Goicochea,² P. Owen,⁵² A. Oyanguren,³⁵ B. K. Pal,⁵⁸ A. Palano,^{13,b} T. Palczewski,²⁷ M. Palutan,¹⁸ J. Panman,³⁷ A. Papanestis,⁴⁸ M. Pappagallo,⁵⁰ C. Parkes,⁵³ C. J. Parkinson,⁵² G. Passaleva,¹⁷ G. D. Patel,⁵¹ M. Patel,⁵² G. N. Patrick,⁴⁸ C. Patrignani,^{19,i} C. Pavel-Nicorescu,²⁸ A. Pazos Alvarez,³⁶ A. Pellegrino,⁴⁰ G. Penso,^{24,l} M. Pepe Altarelli,³⁷ S. Perazzini,^{14,c} E. Perez Trigo,³⁶ A. Pérez-Calero Yzquierdo,³⁵ P. Perret,⁵ M. Perrin-Terrin,⁶ L. Pescatore,⁴⁴ E. Pesen,⁶¹ K. Petridis,⁵² A. Petrolini,^{19,i} A. Phan,⁵⁸ E. Picatoste Olloqui,³⁵ B. Pietrzyk,⁴ T. Pilarč,⁴⁷ D. Pinci,²⁴ S. Playfer,⁴⁹ M. Plo Casasus,³⁶ F. Polci,⁸ G. Polok,²⁵ A. Poluektov,^{47,33} E. Polycarpo,² A. Popov,³⁴ D. Popov,¹⁰ B. Popovici,²⁸ C. Potterat,³⁵ A. Powell,⁵⁴ J. Prisciandaro,³⁸ A. Pritchard,⁵¹ C. Prouve,⁷ V. Pugatch,⁴³ A. Puig Navarro,³⁸ G. Punzi,^{22,r} W. Qian,⁴ J. H. Rademacker,⁴⁵ B. Rakotomiamanana,³⁸ M. S. Rangel,² I. Raniuk,⁴² N. Rauschmayr,³⁷ G. Raven,⁴¹ S. Redford,⁵⁴ M. M. Reid,⁴⁷ A. C. dos Reis,¹ S. Ricciardi,⁴⁸ A. Richards,⁵² K. Rinnert,⁵¹ V. Rives Molina,³⁵ D. A. Roa Romero,⁵ P. Robbe,⁷ D. A. Roberts,⁵⁷ E. Rodrigues,⁵³ P. Rodriguez Perez,³⁶ S. Roiser,³⁷ V. Romanovsky,³⁴ A. Romero Vidal,³⁶

J. Rouvinet,³⁸ T. Ruf,³⁷ F. Ruffini,²² H. Ruiz,³⁵ P. Ruiz Valls,³⁵ G. Sabatino,^{24,h} J. J. Saborido Silva,³⁶ N. Sagidova,²⁹ P. Sail,⁵⁰ B. Saitta,^{15,d} V. Salustino Guimaraes,² B. Sanmartin Sedes,³⁶ M. Sannino,^{19,i} R. Santacesaria,²⁴ C. Santamarina Rios,³⁶ E. Santovetti,^{23,h} M. Sapunov,⁶ A. Sarti,^{18,l} C. Satriano,^{24,m} A. Satta,²³ M. Savrie,^{16,e} D. Savrina,^{30,31} P. Schaack,⁵² M. Schiller,⁴¹ H. Schindler,³⁷ M. Schlupp,⁹ M. Schmelling,¹⁰ B. Schmidt,³⁷ O. Schneider,³⁸ A. Schopper,³⁷ M.-H. Schune,⁷ R. Schwemmer,³⁷ B. Sciascia,¹⁸ A. Sciubba,²⁴ M. Seco,³⁶ A. Semennikov,³⁰ K. Senderowska,²⁶ I. Sepp,⁵² N. Serra,³⁹ J. Serrano,⁶ P. Seyfert,¹¹ M. Shapkin,³⁴ I. Shapoval,^{16,42} P. Shatalov,³⁰ Y. Shcheglov,²⁹ T. Shears,^{51,37} L. Shekhtman,³³ O. Shevchenko,⁴² V. Shevchenko,³⁰ A. Shires,⁹ R. Silva Coutinho,⁴⁷ M. Sirendi,⁴⁶ T. Skwarnicki,⁵⁸ N. A. Smith,⁵¹ E. Smith,^{54,48} J. Smith,⁴⁶ M. Smith,⁵³ M. D. Sokoloff,⁵⁶ F. J. P. Soler,⁵⁰ F. Soomro,³⁸ D. Souza,⁴⁵ B. Souza De Paula,² B. Spaan,⁹ A. Sparkes,⁴⁹ P. Spradlin,⁵⁰ F. Stagni,³⁷ S. Stahl,¹¹ O. Steinkamp,³⁹ S. Stevenson,⁵⁴ S. Stoica,²⁸ S. Stone,⁵⁸ B. Storaci,³⁹ M. Straticiu,²⁸ U. Straumann,³⁹ V. K. Subbiah,³⁷ L. Sun,⁵⁶ S. Swientek,⁹ V. Syropoulos,⁴¹ M. Szczekowski,²⁷ P. Szczypka,^{38,37} T. Szumlak,²⁶ S. T'Jampens,⁴ M. Teklishyn,⁷ E. Teodorescu,²⁸ F. Teubert,³⁷ C. Thomas,⁵⁴ E. Thomas,³⁷ J. van Tilburg,¹¹ V. Tisserand,⁴ M. Tobin,³⁸ S. Tolc,⁴¹ D. Tonelli,³⁷ S. Topp-Joergensen,⁵⁴ N. Torr,⁴ E. Tournefier,^{4,52} S. Tourneur,³⁸ M. T. Tran,³⁸ M. Tresch,³⁹ A. Tsaregorodtsev,⁶ P. Tsopelas,⁴⁰ N. Tuning,⁴⁰ M. Ubeda Garcia,³⁷ A. Ukleja,²⁷ D. Urner,⁵³ A. Ustyuzhanin,^{52,p} U. Uwer,¹¹ V. Vagnoni,¹⁴ G. Valenti,¹⁴ A. Vallier,⁷ M. Van Dijk,⁴⁵ R. Vazquez Gomez,¹⁸ P. Vazquez Regueiro,³⁶ C. Vázquez Sierra,³⁶ S. Vecchi,¹⁶ J. J. Velthuis,⁴⁵ M. Veltri,^{17,g} G. Veneziano,³⁸ M. Vesterinen,³⁷ B. Viaud,⁷ D. Vieira,² X. Vilasis-Cardona,^{35,n} A. Vollhardt,³⁹ D. Volyansky,¹⁰ D. Voong,⁴⁵ A. Vorobyev,²⁹ V. Vorobyev,³³ C. Voß,⁶⁰ H. Voss,¹⁰ R. Waldi,⁶⁰ C. Wallace,⁴⁷ R. Wallace,¹² S. Wandernoth,¹¹ J. Wang,⁵⁸ D. R. Ward,⁴⁶ N. K. Watson,⁴⁴ A. D. Webber,⁵³ D. Websdale,⁵² M. Whitehead,⁴⁷ J. Wicht,³⁷ J. Wiechczynski,²⁵ D. Wiedner,¹¹ L. Wiggers,⁴⁰ G. Wilkinson,⁵⁴ M. P. Williams,^{47,48} M. Williams,⁵⁵ F. F. Wilson,⁴⁸ J. Wimberley,⁵⁷ J. Wishahi,⁹ W. Wislicki,²⁷ M. Witek,²⁵ S. A. Wotton,⁴⁶ S. Wright,⁴⁶ S. Wu,³ K. Wyllie,³⁷ Y. Xie,^{49,37} Z. Xing,⁵⁸ Z. Yang,³ R. Young,⁴⁹ X. Yuan,³ O. Yushchenko,³⁴ M. Zangoli,¹⁴ M. Zavertyaev,^{10,a} F. Zhang,³ L. Zhang,⁵⁸ W. C. Zhang,¹² Y. Zhang,³ A. Zhelezov,¹¹ A. Zhokhov,³⁰ L. Zhong,³ and A. Zvyagin³⁷

(LHCb Collaboration)

¹Centro Brasileiro de Pesquisas Físicas (CBPF), Rio de Janeiro, Brazil²Universidade Federal do Rio de Janeiro (UFRJ), Rio de Janeiro, Brazil³Center for High Energy Physics, Tsinghua University, Beijing, China⁴LAPP, Université de Savoie, CNRS/IN2P3, Annecy-Le-Vieux, France⁵Clermont Université, Université Blaise Pascal, CNRS/IN2P3, LPC, Clermont-Ferrand, France⁶CPPM, Aix-Marseille Université, CNRS/IN2P3, Marseille, France⁷LAL, Université Paris-Sud, CNRS/IN2P3, Orsay, France⁸LPNHE, Université Pierre et Marie Curie, Université Paris Diderot, CNRS/IN2P3, Paris, France⁹Fakultät Physik, Technische Universität Dortmund, Dortmund, Germany¹⁰Max-Planck-Institut für Kernphysik (MPIK), Heidelberg, Germany¹¹Physikalisches Institut, Ruprecht-Karls-Universität Heidelberg, Heidelberg, Germany¹²School of Physics, University College Dublin, Dublin, Ireland¹³Sezione INFN di Bari, Bari, Italy¹⁴Sezione INFN di Bologna, Bologna, Italy¹⁵Sezione INFN di Cagliari, Cagliari, Italy¹⁶Sezione INFN di Ferrara, Ferrara, Italy¹⁷Sezione INFN di Firenze, Firenze, Italy¹⁸Laboratori Nazionali dell'INFN di Frascati, Frascati, Italy¹⁹Sezione INFN di Genova, Genova, Italy²⁰Sezione INFN di Milano Bicocca, Milano, Italy²¹Sezione INFN di Padova, Padova, Italy²²Sezione INFN di Pisa, Pisa, Italy²³Sezione INFN di Roma Tor Vergata, Roma, Italy²⁴Sezione INFN di Roma La Sapienza, Roma, Italy²⁵Henryk Niewodniczanski Institute of Nuclear Physics Polish Academy of Sciences, Kraków, Poland²⁶AGH-University of Science and Technology, Faculty of Physics and Applied Computer Science, Kraków, Poland²⁷National Center for Nuclear Research (NCBJ), Warsaw, Poland²⁸Horia Hulubei National Institute of Physics and Nuclear Engineering, Bucharest-Magurele, Romania²⁹Petersburg Nuclear Physics Institute (PNPI), Gatchina, Russia

- ³⁰*Institute of Theoretical and Experimental Physics (ITEP), Moscow, Russia*
- ³¹*Institute of Nuclear Physics, Moscow State University (SINP MSU), Moscow, Russia*
- ³²*Institute for Nuclear Research of the Russian Academy of Sciences (INR RAN), Moscow, Russia*
- ³³*Budker Institute of Nuclear Physics (SB RAS) and Novosibirsk State University, Novosibirsk, Russia*
- ³⁴*Institute for High Energy Physics (IHEP), Protvino, Russia*
- ³⁵*Universitat de Barcelona, Barcelona, Spain*
- ³⁶*Universidad de Santiago de Compostela, Santiago de Compostela, Spain*
- ³⁷*European Organization for Nuclear Research (CERN), Geneva, Switzerland*
- ³⁸*Ecole Polytechnique Fédérale de Lausanne (EPFL), Lausanne, Switzerland*
- ³⁹*Physik-Institut, Universität Zürich, Zürich, Switzerland*
- ⁴⁰*Nikhef National Institute for Subatomic Physics, Amsterdam, The Netherlands*
- ⁴¹*Nikhef National Institute for Subatomic Physics and VU University Amsterdam, Amsterdam, The Netherlands*
- ⁴²*NSC Kharkiv Institute of Physics and Technology (NSC KIPT), Kharkiv, Ukraine*
- ⁴³*Institute for Nuclear Research of the National Academy of Sciences (KINR), Kyiv, Ukraine*
- ⁴⁴*University of Birmingham, Birmingham, United Kingdom*
- ⁴⁵*H.H. Wills Physics Laboratory, University of Bristol, Bristol, United Kingdom*
- ⁴⁶*Cavendish Laboratory, University of Cambridge, Cambridge, United Kingdom*
- ⁴⁷*Department of Physics, University of Warwick, Coventry, United Kingdom*
- ⁴⁸*STFC Rutherford Appleton Laboratory, Didcot, United Kingdom*
- ⁴⁹*School of Physics and Astronomy, University of Edinburgh, Edinburgh, United Kingdom*
- ⁵⁰*School of Physics and Astronomy, University of Glasgow, Glasgow, United Kingdom*
- ⁵¹*Oliver Lodge Laboratory, University of Liverpool, Liverpool, United Kingdom*
- ⁵²*Imperial College London, London, United Kingdom*
- ⁵³*School of Physics and Astronomy, University of Manchester, Manchester, United Kingdom*
- ⁵⁴*Department of Physics, University of Oxford, Oxford, United Kingdom*
- ⁵⁵*Massachusetts Institute of Technology, Cambridge, Massachusetts, USA*
- ⁵⁶*University of Cincinnati, Cincinnati, Ohio, USA*
- ⁵⁷*University of Maryland, College Park, Maryland, USA*
- ⁵⁸*Syracuse University, Syracuse, New York, USA*
- ⁵⁹*Pontifícia Universidade Católica do Rio de Janeiro (PUC-Rio), Rio de Janeiro, Brazil [associated with Universidade Federal do Rio de Janeiro (UFRJ), Rio de Janeiro, Brazil]*
- ⁶⁰*Institut für Physik, Universität Rostock, Rostock, Germany [associated with Physikalisches Institut, Ruprecht-Karls-Universität Heidelberg, Heidelberg, Germany]*
- ⁶¹*Celal Bayar University, Manisa, Turkey [associated with European Organization for Nuclear Research (CERN), Geneva, Switzerland]*

^aAlso at P.N. Lebedev Physical Institute, Russian Academy of Science (LPI RAS), Moscow, Russia.

^bAlso at Università di Bari, Bari, Italy.

^cAlso at Università di Bologna, Bologna, Italy.

^dAlso at Università di Cagliari, Cagliari, Italy.

^eAlso at Università di Ferrara, Ferrara, Italy.

^fAlso at Università di Firenze, Firenze, Italy.

^gAlso at Università di Urbino, Urbino, Italy.

^hAlso at Università di Modena e Reggio Emilia, Modena, Italy.

ⁱAlso at Università di Genova, Genova, Italy.

^jAlso at Università di Milano Bicocca, Milano, Italy.

^kAlso at Università di Roma Tor Vergata, Roma, Italy.

^lAlso at Università di Roma La Sapienza, Roma, Italy.

^mAlso at Università della Basilicata, Potenza, Italy.

ⁿAlso at LIFAELS, La Salle, Universitat Ramon Llull, Barcelona, Spain.

^oAlso at Hanoi University of Science, Hanoi, Vietnam.

^pAlso at Institute of Physics and Technology, Moscow, Russia.

^qAlso at Università di Padova, Padova, Italy.

^rAlso at Università di Pisa, Pisa, Italy.

^sAlso at Scuola Normale Superiore, Pisa, Italy.